Available online at www.sciencedirect.com
ScienceDirect
C. R. Mecanique 337 (2009) 198–207
COMPTES RENDUS MECANIQUE

Transmission loss of multilayer panels containing a fluid using progressive wave model: Comparison with impedance progressive model and experiments

N. Mohammadi, M.J. Mahjoob *

NVA Research Centre, School of Mechanical Engineering, University of Tehran, Tehran, Iran

Received 12 October 2008; accepted after revision 2 May 2009

Available online 22 May 2009

Abstract

The progressive wave model is applied to calculate transmission loss (TL) of triple layer panels. Theoretical values are then compared with impedance progressive model and experimental results. The triple layer panel comprises two solid layers with a middle layer of air or liquid. An impedance tube is employed to measure the TL values experimentally. The comparison of the two analytical models shows that the results of both models are relatively close. However, the progressive wave model leads to slightly larger values for a wide range of frequencies. Also, for the case of an air middle layer, a shift of the resonances to higher frequencies is observed in the results of the progressive wave model. Computational results also demonstrate that applying a liquid middle layer (replacing air) significantly improves the performance of the acoustic panel particularly at frequencies below 4000 rad/s (640 Hz). Shifting resonance frequencies to higher frequencies is another advantage of incorporating the liquid layer. Good agreement was also found between theoretical and experimental results. ***To cite this article: N. Mohammadi, M.J. Mahjoob, C. R. Mecanique 337 (2009).***

Keywords: Acoustic insulation; Multilayer acoustic panels; Transmission loss; Impedance tube

1. Introduction

Multilayer acoustic panels are extensively used as sound barriers in buildings, and in the automotive and aerospace industries. The classical models to predict transmission loss (TL) of multilayer panels are the impedance progressive model (IPM), progressive wave model (PWM) and multiple reflection model (MRM).

Beranek and Work [1] used the IPM and calculated the TL of a double layer panel with air space, in a normal incidence field. They used impervious layers with different impedance values [2]. They also studied the influence of absorptive materials used inside the air space on the TL values. Mangiarotty [3] studied the TL of an airplane's body modeled as a double layer panel, applying the IPM. He improved the TL value with the change of layers surface

* Corresponding author.
E-mail addresses: nmohamady@ut.ac.ir (N. Mohammadi), mmahjoob@ut.ac.ir (M.J. Mahjoob).

1631-0721/$ – see front matter
doi:10.1016/j.crme.2009.05.001

density, change in the air gap and use of absorptive materials in the air space (air cavity). Mulholland et al. [4] generalized the model presented by Beranek [1] for a random incidence field.

London [5] studied the TL of a double layer panel in a random incidence field using the PWM and then compared it with experiments. Layers were exactly identical and the impedance of each layer was determined experimentally. The results showed that employing absorptive materials in the air cavity was advantageous only when the layers were relatively light.

Mulholland et al. [6] derived the MRM to estimate the TL of a double layer panel in random incidence field. They showed that taking the sound energy absorbed by each layer into consideration brings good conformity between theory and experiments. One could easily include absorptive materials used in the air space in this model.

Tadeu et al. [7] compared the theoretical TL of single and double layer panels predicted by other researchers with their own experimental results. Test samples were placed at the opening between two standard rooms. Good agreements were reported between experimental and theoretical results except at frequencies lower than 200 Hz and for a sample area smaller than 0.36 m^2. Resonance phenomena at low frequencies also increase the deviation between experimental and theoretical data.

In a previous work of the authors [8], the TL of a triple layer panel with middle fluid layer was calculated using IPM. Herein, the PWM is developed to predict the TL of the triple layer panel with a middle layer of Newtonian fluid. The computational results of the two models are then compared and analyzed. Experiments are also conducted with the impedance tube used previously [8]. The two-load method is used in the experiments due to its superior performance, the details of which will be discussed.

2. Theoretical model

Here, the PWM has been used to calculate the TL. Combining wave propagation equations in air and fluid, momentum equations for the solid layers and boundary conditions (continuity of velocity for air and fluid particles at interfaces), the ratio of incident wave pressure to the transmitted wave is determined. The TL of the panel is then calculated.

2.1. Acoustical wave propagation in a viscous Newtonian fluid

The equation governing sound propagation in a Newtonian fluid is obtained utilizing the three basic equations: conservation of mass, conservation of momentum and equation of state. The sound wave equation for a viscous fluid is as follows:

$$\frac{4\nu}{3c_0^2}p_{xxt} + p_{xx} - \frac{1}{c_0^2}p_{tt} = 0 \tag{1}$$

assuming Stoke's condition $\lambda = \frac{-2}{3}\mu$. Here, c_0 and ν are sound velocity in the fluid and fluid kinematic viscosity, respectively. Subscripts t and x denote derivatives of sound pressure with respect to time and distance.

The complex form of the time-harmonic solution of sound wave pressure can thus be written as, [8]:

$$p = \mathrm{e}^{\mathrm{j}\omega t}\left[P_0^+\mathrm{e}^{-\mathrm{j}k_0 x} + P_0^-\mathrm{e}^{\mathrm{j}k_0 x}\right] \tag{2}$$

where

$$k_0 = k_R + \mathrm{j}k_I, \quad k_R, k_I = \pm\frac{\omega}{c_0}\chi^{-1/4}\left[\frac{1 \pm \chi^{-1/2}}{2}\right]^{1/2}, \quad \chi = 1 + \left(\frac{4\nu\omega}{3c_0^2}\right)^2 \tag{3}$$

2.2. Infinite triple layer acoustic panels

Fig. 1 shows the triple-layered acoustic panel considered.

Now, the sound wave equations in regions (1), (2) and (3) are in the following forms:

$$\begin{aligned}
p_1 &= \mathrm{e}^{\mathrm{j}\omega t}\left[P_i\mathrm{e}^{-\mathrm{j}k(x\cos\theta + y\sin\theta)} + P_r\mathrm{e}^{\mathrm{j}k(x\cos\theta - y\sin\theta)}\right] \\
p_2 &= \mathrm{e}^{\mathrm{j}\omega t}\left[A\mathrm{e}^{-\mathrm{j}k_0(x\cos\theta_0 + y\sin\theta_0)} + B\mathrm{e}^{\mathrm{j}k_0(x\cos\theta_0 - y\sin\theta_0)}\right] \\
p_3 &= \mathrm{e}^{\mathrm{j}\omega t}P_t\mathrm{e}^{-\mathrm{j}k(x\cos\theta + y\sin\theta)}
\end{aligned} \tag{4}$$

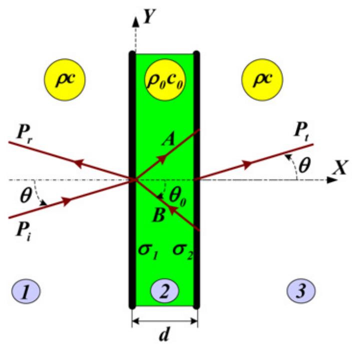

Fig. 1. Schematic sketch of the triple layer panel considered.

The pressure amplitude ratio (i.e. the wave pressure incident on the panel to the wave pressure transmitted from it) can be derived by combining the momentum equations for the layers along with the boundary conditions. This ratio is computed for same 'y' values; therefore, it does not appear in the formulations. The momentum equation for an air element at $x = 0$ and $x = d$ is as follows:

$$-\frac{\partial p_1}{\partial x} = \rho \dot{u}_{1x} = \mathrm{j}\omega\rho u_{1x}, \quad \text{at } x = 0$$
$$-\frac{\partial p_3}{\partial x} = \rho \dot{u}_{3x} = \mathrm{j}\omega\rho u_{3x}, \quad \text{at } x = d \tag{5}$$

where u_i refers to the particle velocity in region (i). Similarly, momentum equation of a fluid element at $x = 0$ and $x = d$ can be written as:

$$-\frac{\partial p_2}{\partial x} = \rho_0 \dot{u}_{2x} = \mathrm{j}\omega\rho_0 u_{2x}, \quad \text{at } x = 0$$
$$-\frac{\partial p_2}{\partial x} = \rho_0 \dot{u}_{2x} = \mathrm{j}\omega\rho_0 u_{2x}, \quad \text{at } x = d \tag{6}$$

Eqs. (5) and (6) and boundary conditions (i.e. the velocity continuity of air/fluid particles at the layers interfaces) imply:

$$\frac{1}{\rho}\frac{\partial p_1}{\partial x} = \frac{1}{\rho_0}\frac{\partial p_2}{\partial x}, \quad \text{at } x = 0$$
$$\frac{1}{\rho_0}\frac{\partial p_2}{\partial x} = \frac{1}{\rho}\frac{\partial p_3}{\partial x}, \quad \text{at } x = d \tag{7}$$

From Eqs. (4)–(7):

$$(P_i - P_r)\rho_0 k \cos\theta = (A - B)\rho k_0 \cos\theta_0 \tag{8}$$

also

$$A\mathrm{e}^{-\mathrm{j}k_0 d\cos\theta_0} - B\mathrm{e}^{\mathrm{j}k_0 d\cos\theta_0} = P_t \frac{\rho_0 k\cos\theta}{\rho k_0\cos\theta_0}\mathrm{e}^{-\mathrm{j}kd\cos\theta} \tag{9}$$

The equation of motion of the first solid layer is:

$$p_1 - p_2 = Z_1 V_1 = \mathrm{j}\omega\sigma_1 V_1, \quad \text{at } x = 0 \tag{10}$$

and for the second solid layer:

$$p_2 - p_3 = Z_2 V_2 = \mathrm{j}\omega\sigma_2 V_2, \quad \text{at } x = d \tag{11}$$

Z_i indicates the impedance and V_i the velocity of the layer (i). The velocity of each layer is the same as the velocity of fluid or air particles adjacent to that layer. Therefore, from Eqs. (4)–(6), (10) and (11):

$$(P_i + P_r) - (A + B) = \frac{Z_1\cos\theta}{\rho c}(P_i - P_r) \tag{12}$$

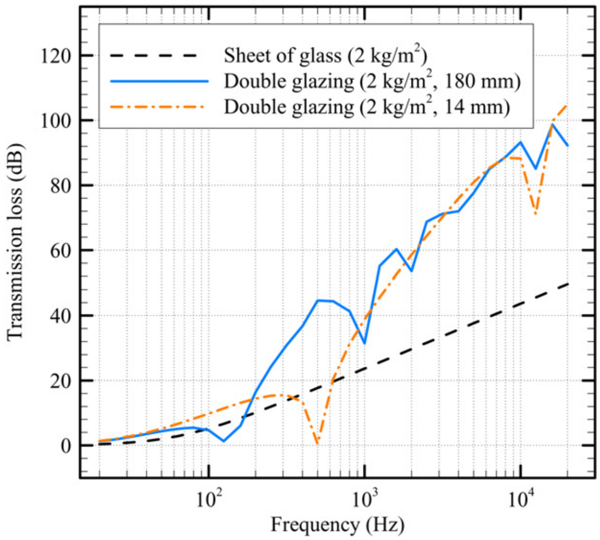

Fig. 2. Theoretical TL values predicted for a sheet of glass ($2\ \text{kg/m}^2$), a double glazed window consisting of two glass sheets ($2\ \text{kg/m}^2$) with middle layers of air ($d = 180$ mm and $d = 14$ mm).

also

$$A\mathrm{e}^{-\mathrm{j}k_0 d\cos\theta_0} + B\mathrm{e}^{\mathrm{j}k_0 d\cos\theta_0} = \left(1 + \frac{Z_2\cos\theta}{\rho c}\right) P_t \mathrm{e}^{-\mathrm{j}kd\cos\theta} \tag{13}$$

From Eqs. (8), (9), (12) and (13) the pressure amplitude ratio is obtained as follows:

$$\frac{P_i}{P_t} = \frac{1}{4}\frac{\beta}{\beta_0}\left[(1+\psi)\left(\frac{\rho_0}{\rho} + \psi_0\right)\mathrm{e}^{\mathrm{j}(\beta_0-\beta)} - (1-\psi)\left(\frac{\rho_0}{\rho} - \psi_0\right)\mathrm{e}^{-\mathrm{j}(\beta_0+\beta)}\right] \tag{14}$$

where

$$\begin{gathered} \psi_0 = (1+2\gamma_2)\frac{\beta_0}{\beta}, \quad \psi = (1+2\gamma_1)\frac{\rho\beta_0}{\rho_0\beta} \\ \gamma_1 = \frac{1}{2}\frac{Z_1\cos\theta}{\rho c}, \quad \gamma_2 = \frac{1}{2}\frac{Z_2\cos\theta}{\rho c}, \quad \beta_0 = k_0 d\cos\theta_0, \quad \beta = kd\cos\theta \end{gathered} \tag{15}$$

The coefficient of sound transmission for an acoustic panel can be written as:

$$\tau(\omega) = \left|\frac{P_t}{P_i}\right|^2 \tag{16}$$

As a result, the TL is calculated as:

$$\mathrm{TL} = 10\log_{10}\left(\frac{1}{\tau(\omega)}\right) \tag{17}$$

As a numerical example, the problem mentioned in [9], p. 95, is solved with the presented method. The TL for a 500 Hz sound wave passing normally through a sheet of glass with a mass of $2\ \text{kg/m}^2$ is calculated first ($d = 0$ in our equations, which exactly coincides with the classical solution; Eq. (4.7) in the same reference). Then a doubled glazed window is examined for its transmission loss. Two sheets of the same glass with a gap of $d = 180$ mm are installed. The result of our solution is plotted in Fig. 2. As it is expected, the normally incident wave is most effectively stopped at 500 Hz where a 41 dB loss is achieved. However, since the gap is usually much less in practice, transmission loss of double glazing with 14 mm gap is also computed (see the results in the same figure). A TL of 0.4 dB shows the worse situation where the resonance at 500 Hz has degraded the performance of the double insulator drastically.

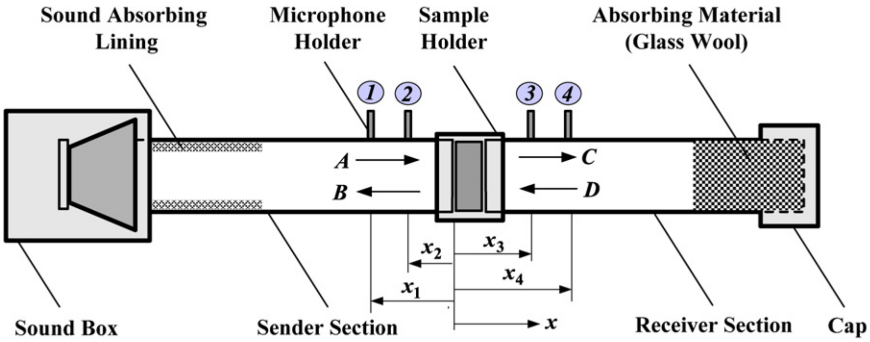

Fig. 3. Schematic structure of the device (modified impedance tube) made for the TL measurement.

3. Experimental procedure

Impedance tubes have been extensively used to measure the TL of different materials in recent years. The impedance tube method is approximate and much less expensive requiring little space compared to the traditional two-room method. The experiments here are based on measurements by an impedance tube designed and constructed to validate the theoretical results [8].

3.1. Theory

The theory has been established based on the transfer matrix method. Fig. 3 shows a schematic structure of the modified impedance tube device made for the TL measurements.

Relations between sound pressure amplitudes ($A - D$) and complex values of sound pressure at four measuring stations of microphones ($p_1 - p_4$) are obtained as [10]:

$$A = \sqrt{G_{rr}}\frac{\mathrm{j}}{2}\frac{H_{p_1 r}\mathrm{e}^{\mathrm{j}kx_2} - H_{p_2 r}\mathrm{e}^{\mathrm{j}kx_1}}{\sin k(x_1 - x_2)}, \qquad B = \sqrt{G_{rr}}\frac{-\mathrm{j}}{2}\frac{H_{p_1 r}\mathrm{e}^{-\mathrm{j}kx_2} - H_{p_2 r}\mathrm{e}^{-\mathrm{j}kx_1}}{\sin k(x_1 - x_2)}$$
$$C = \sqrt{G_{rr}}\frac{\mathrm{j}}{2}\frac{H_{p_3 r}\mathrm{e}^{\mathrm{j}kx_4} - H_{p_4 r}\mathrm{e}^{\mathrm{j}kx_3}}{\sin k(x_3 - x_4)}, \qquad D = \sqrt{G_{rr}}\frac{-\mathrm{j}}{2}\frac{H_{p_3 r}\mathrm{e}^{-\mathrm{j}kx_4} - H_{p_4 r}\mathrm{e}^{-\mathrm{j}kx_3}}{\sin k(x_3 - x_4)} \tag{18}$$

where $H_{p_i r} = \frac{G_{p_i r}}{G_{rr}}$ are frequency response functions. G_{rr} and $G_{p_i r}$ are the averaged, one-sided auto spectrum density function of the reference signal, r, and the averaged, one-sided cross spectrum density function of the reference signal and signal p_i, respectively.

Two different methods have been presented to analyze the measured pressure for the TL calculation, i.e. anechoic termination [11,12] and two-load methods [13–15]. Selection of the proper method depends upon the specific design of the test tube and test materials.

In this study, the two-load method is used the basis of which will be explained later. Tests are carried out with (and without) applying absorptive materials inside the right end of the receiver section (see Fig. 3).

3.2. Test setup

The same impedance tube made for the previous investigation was used here. The experimental setup is shown schematically in Fig. 4. The details can be found in [8]. Slight changes were made to upgrade the measurement setup. The main improvement was adding a sound absorbing lining, 20 cm long, applied to the internal surface of the tube at the speaker side (see Fig. 3).

Five test samples were made (Fig. 5): lead, steel, plywood, liquid (nano-ferrofluid), and air-filled Pyrex glass tube. The first three samples were made in order to calibrate the tube with the results supplied by BHRC (Building and Housing Research Center) obtained with an original B&K 4206 impedance tube. The fluid specimens were made of a Pyrex glass tube with 30 mm length, outer diameter 38 mm and 1.5 mm wall thickness, filled with water, oil, and the nano-ferrofluid.

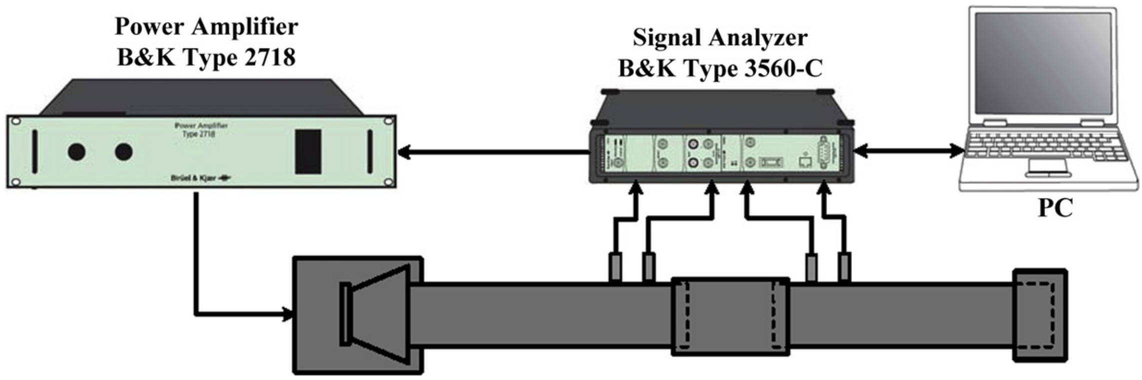

Fig. 4. Test equipment and setup.

Fig. 5. Sample holder (top) and test specimens (bottom: from left to right: lead, steel, plywood, nano-ferrofluid and air-filled Pyrex tube).

3.3. Test procedure

In the experimental work, the TL values of the three common materials including steel, plywood and lead are measured first. Test specimens are disks with similar diameters and different lengths. Both measurement methods are examined here, including two-load and anechoic termination with different boundary conditions at the tube termination. The boundary conditions examined are: tube end with/without cap, with/without absorbent material inside and with different lengths of absorbent material. Comparison is then made with the B&K tube mentioned previously. The observations show better agreement with the results obtained by the two-load method.

The rest of the experiments are therefore conducted using two-load method. An averaged value of the results obtained for different boundary conditions will be reported here as the outcome of several experiments. These results will be given in Section 4.2, together with the theoretical ones, for comparison.

4. Results

4.1. Theoretical results

The theoretical TL values of a triple layer panel with middle layer of air, oil, water and nano-ferrofluid (NMF-128DV) were calculated. For a comparison with the impedance tube, an incidence angle of $\theta = 0$ is applied in the computations. The results are shown for $1/3$ Octave bands for different distances of the layers and various layer (wall) thicknesses (see Figs. 6 to 8). The material data used in Eqs. (14) and (15) for glass as well as air, oil and nano-ferrofluid are listed in Table 1.

According to Fig. 6, the acoustic performance of the triple layer panel with air space is good at the frequency range above 5000 $\mathrm{rad/s}$ (780 Hz). The use of a liquid as middle layer increases the TL over the entire frequency range.

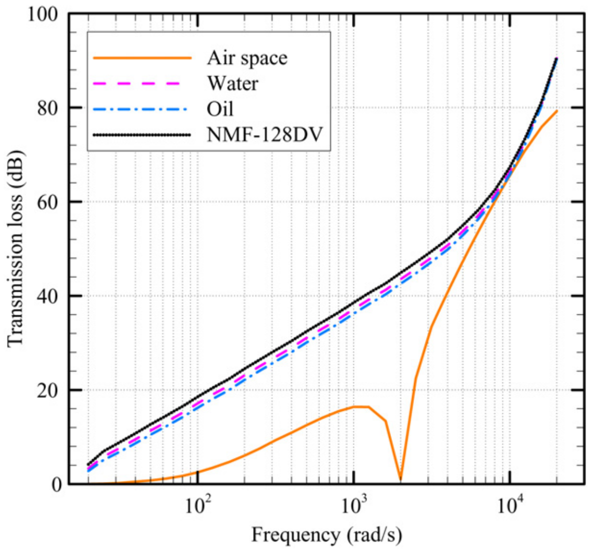

Fig. 6. Theoretical TL values predicted for a triple layer panel consisting of two glass walls (1.5 mm and 1.5 mm) with middle layers of air, oil, water and NMF-128DV ($d = 30$ mm).

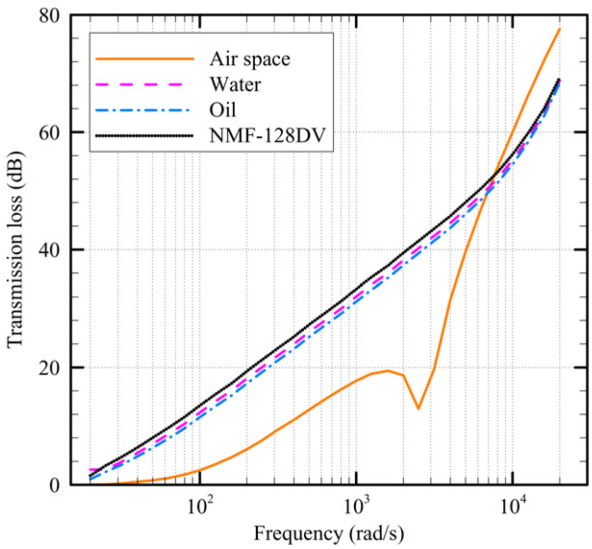

Fig. 7. Theoretical TL values predicted for a triple layer panel consisting of two glass walls (1.5 mm and 1.5 mm) with middle layers of air, oil, water and NMF-128DV ($d = 15$ mm).

Table 1
Material data used for glass, air, water, oil and nano-ferrofluid (NMF-128DV).

	ρ_0 (kg m^{-3})	c_0 (m s^{-1})	μ (N s m^{-2})	σ (kg m^{-2})
Glass-Pyrex	N/A	N/A	N/A	3.36
NMF-128DV	1.2×10^3	1.23×10^3	3.53×10^{-2}	N/A
Oil	8.8×10^2	1.7×10^3	3.7×10^{-1}	N/A
Water	1.0×10^3	1.48×10^3	9.79×10^{-4}	N/A
Air	1.2	344	1.81×10^{-5}	N/A

At low frequencies, especially below 4000 rad/s (640 Hz), where the performance of middle air layer is poor, the liquid layer provides desirable performance. Fluid density affects the TL values more than other parameters, i.e. the wave velocity and the kinematic viscosity. Hence the TL of a triple layer panel with middle layers of water, oil, and nano-ferrofluid are close to each other. The application of the liquid layer increases the resonance frequencies and shifts them to higher frequencies which might be an advantage.

Fig. 7 shows that a decrease in the layers gap reduces the TL values over a wide frequency range. In the case of air space, such a reduction leads to an increase in the mass-air-mass resonance frequency.

Comparing Figs. 6 and 8, the TL enhances for a wide range of frequencies once the wall surface density is increased. Similarly, changes in the surface density of walls shift the mass-air-mass resonance frequency.

In Fig. 9, a comparison between IPM [8] and PWM is showed. The results of both models are close. However, PWM leads to slightly larger values for a wide range of frequencies. Also, in the case of air gap, a shift of the resonances to higher frequencies is observed in PWM results.

4.2. Test results

The experimental results for TL values re-plotted in Figs. 10 to 13 within the working frequency range. Plots of theoretical values are also included in the figures. Good agreement is obtained between theoretical findings and experiments over the entire frequency range.

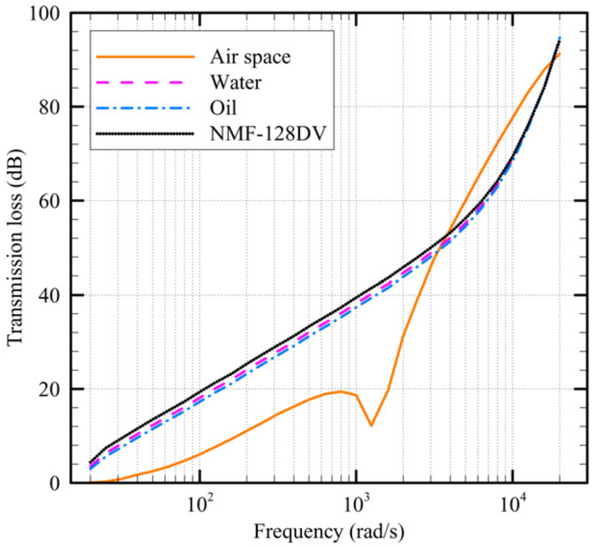

Fig. 8. Theoretical TL values predicted for a triple layer panel consisting of two glass walls (3 mm and 3 mm) with middle layers of air, oil, water and NMF-128DV ($d = 30$ mm).

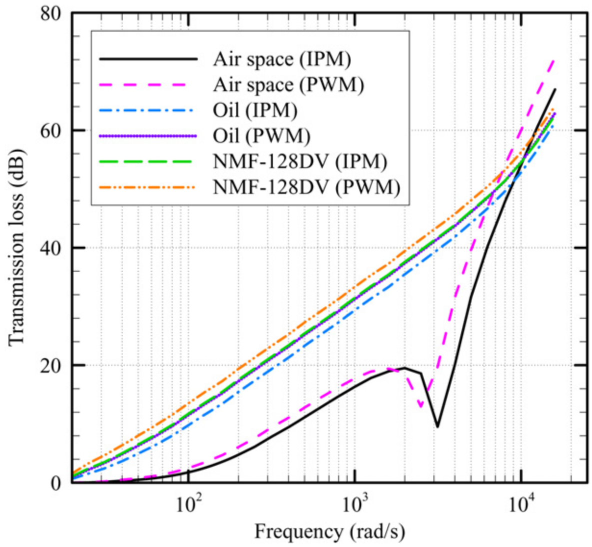

Fig. 9. Theoretical TL values predicted for a triple layer panel consisting of two glass walls (1.5 mm and 1.5 mm) with middle layers of air, oil and NMF-128DV ($d = 15$ mm): Comparison between IPM [8] and PWM.

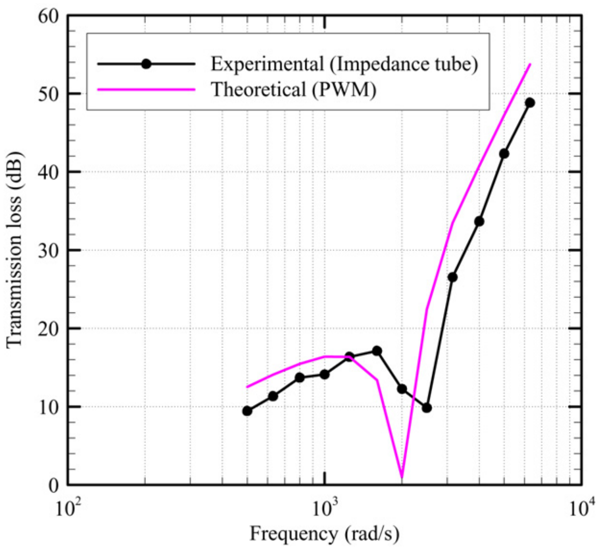

Fig. 10. A comparison of theoretical and experimental TL values for a triple layer panel consisting of two glass walls (1.5 mm and 1.5 mm) with the middle layer of air ($d = 30$ mm).

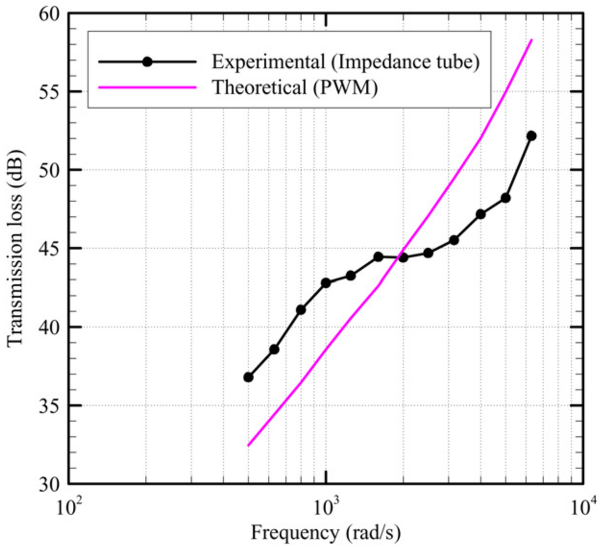

Fig. 11. A comparison of theoretical and experimental TL values for a triple layer panel consisting of two glass walls (1.5 mm and 1.5 mm) with the middle layer of NMF-128DV ($d = 30$ mm).

5. Concluding remarks

A method was presented to predict the TL of triple layer panels with a middle layer of Newtonian fluid. The development was based on the PWM. Computational results were then compared with the values obtained by the IPM of the earlier work and the experimental results. Acoustic performance of panels containing air, oil, water and a ferromagnetic nano-particles fluid (nano-ferrofluid) was evaluated theoretically. The study was conducted for various gaps between sidewalls as well as different wall thicknesses. The addition of fluid (liquid) layer led to considerable increase of the TL, especially at frequencies below 4000 rad/s (640 Hz). Also noticed was the elimination of low resonance

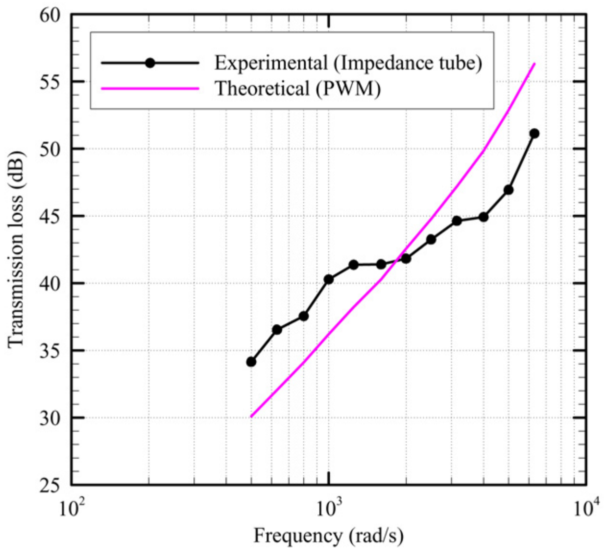

Fig. 12. A comparison of theoretical and experimental TL values for a triple layer panel consisting of two glass walls (1.5 mm and 1.5 mm) with the middle layer of oil ($d = 30$ mm).

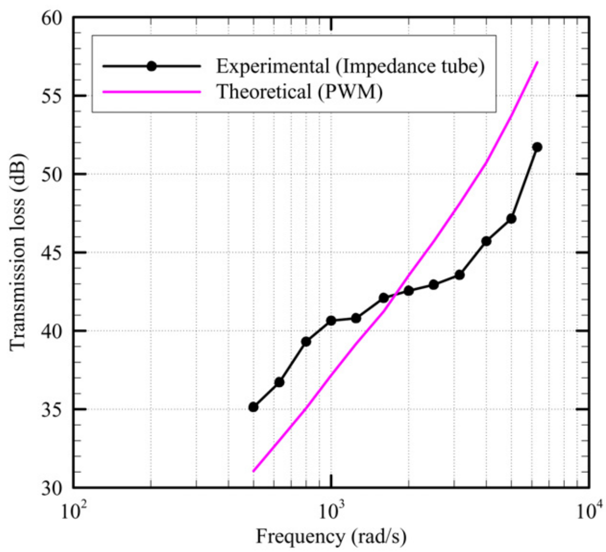

Fig. 13. A comparison of theoretical and experimental TL values for a triple layer panel consisting of two glass walls (1.5 mm and 1.5 mm) with the middle layer of water ($d = 30$ mm).

frequencies; they virtually moved to much higher frequencies. Fluid density is an influential parameter in calculating the TL values. In fact, acoustic panels with different fluids of similar densities result in a similar performance. Increasing the middle gap led to an increase of the TL values and a decrease in resonance frequencies.

Both analytical models examined led to similar results. However, the values computed with PWM were slightly higher. Additionally, the computational results for the case of air middle layer showed a shift of the resonances to higher frequencies.

In order to verify the model experimentally, the previously made impedance tube was employed for the TL measurements. The apparatus was calibrated with the disk samples of known materials. The results were studied applying different boundary conditions for the tube termination. The results of the two-load procedure were preferred. The two-load method was then used in the experiments for the triple layer panel, due to its superior performance. Good agreement between theoretical computations and experimental results was achieved within the test limits.

References

[1] L.L. Beranek, G.A. Work, Sound transmission through multiple structures containing flexible blankets, Journal of the Acoustical Society of America 21 (4) (1949) 419–428.

[2] L.L. Beranek, Acoustical properties of homogeneous, isotropic rigid tiles and flexible blankets, Journal of the Acoustical Society of America 19 (4) (1947) 556–568.

[3] R.A. Mangiarotty, Optimization of the mass distribution and the air spaces in multiple-element soundproofing structures, Journal of the Acoustical Society of America 35 (7) (1963) 1023–1029.

[4] K.A. Mulholland, A.J. Price, H.D. Parbrook, Transmission loss of multiple panels in a random incidence field, Journal of the Acoustical Society of America 43 (6) (1968) 1432–1435.

[5] A. London, Transmission of reverberant sound through double walls, Journal of the Acoustical Society of America 22 (2) (1950) 270–279.

[6] K.A. Mulholland, H.D. Parbrook, A. Cummings, The transmission loss of double panels, Journal of Sound and Vibration 6 (3) (1967) 324–334.

[7] A. Tadeu, J. Antonio, D. Mateus, Sound insulation provided by single and double panel walls—a comparison of analytical solutions versus experimental results, Applied Acoustics 65 (2004) 15–29.

[8] M.J. Mahjoob, N. Mohammadi, S. Malakooti, An investigation into the acoustic insulation of triple-layered panels containing Newtonian fluids: Theory and experiment, Applied Acoustics 70 (1) (2009) 165–171.

[9] A.P. Dowling, J.E. Ffowcs Williams, Sound and Sources of Sound, Ellis Horwood Limited, England, 1983.

[10] O. Olivieri, J.S. Bolton, T. Yoo, Measurement of transmission loss of materials using a standing wave tube, in: Proceedings NOISE-CON 2006, Honolulu, Hawaii, USA, 2006.

[11] B.H. Song, J.S. Bolton, A transfer-matrix approach for estimating the characteristic impedance and wave numbers of limp and rigid porous materials, Journal of the Acoustical Society of America 107 (3) (2000) 1131–1152.

[12] B.H. Song, J.S. Bolton, Y.J. Kang, Effect of circumferential edge constraint on the acoustical properties of glass fiber materials, Journal of the Acoustical Society of America 110 (6) (2001) 2902–2916.
[13] C.J. Young, M.J. Crocker, Prediction of transmission loss in mufflers by the finite-element method, Journal of the Acoustical Society of America 57 (1) (1975) 144–148.
[14] M.L. Munjal, A.G. Doige, Theory of a two source-location method for direct experimental evaluation of the four-pole parameters of an aeroacoustic element, Journal of Sound and Vibration 141 (2) (1990) 323–333.
[15] G. Pispola, K.V. Horoshenkov, F. Asdrubali, Transmission loss measurement of consolidated granular media (L), Journal of the Acoustical Society of America 117 (5) (2005) 2716–2719.